Electron Scattering at Epitaxial Ni(001) Surfaces

Erik Milosevic, Pengyuan Zheng, and Daniel Gall

Abstract— Epitaxial Ni(001) layers are sputter deposited on MgO(001) substrates and their electrical resistivity ρ measured in situ as a function of thickness $d_{Ni} = 5 - 100$ nm to quantify the resistivity size effect due to electron surface scattering. X-ray diffraction θ -2 θ scans, ω -rocking curves, and pole figures confirm an epitaxial layer-substrate relationship with Ni[001] | MgO[001] and Ni[100] MgO[100]. The resistivity is well described with the semi-classical model by Fuchs and Sondheimer and a roomtemperature bulk resistivity $\rho_0 = 7.04 \, \mu\Omega$ cm, yielding a bulk electron mean free path $\lambda = 26 \pm 2$ and 350 ± 20 nm at 295 and 77 K, respectively. Air exposure causes a resistivity increase by up to 21% which is attributed to monolayer surface oxidation that results in a transition from 30% specular to completely diffuse electron surface scattering. All measured data are consistent with a temperature-independent product $\rho_0 \lambda = 18.3 \times 10^{-16} \ \Omega \text{m}^2$ which is 4.5 times larger than previously predicted from first-principles, indicating that Ni is less promising as a metal for narrow interconnect lines than those predictions suggest.

Index Terms—Interconnects, Nickel, BEOL, MOL, Resistivity Scaling, Mean Free Path, Surface Scattering, Alternative Metals

I. INTRODUCTION

major challenge [1], [2] for the continued downscaling and Acorresponding increasing performance of modern integrated circuits is the well-known resistivity size effect in metallic conductors [3], [4]. As the physical dimensions of interconnects decrease, their resistivity increases due to electron scattering at surfaces [5]-[9] and grain boundaries [10]–[16], as commonly described by the classical models by Fuchs and Sondheimer (FS) [17], [18] and Mayadas and Shatzkes (MS) [10], [19], respectively. In addition, surface roughness exacerbates this resistivity size effect [20]-[23]. Both the FS and MS models predict a resistivity increase that is proportional to $\rho_0 \lambda/d$, where ρ_0 is the bulk resistivity, λ is the bulk electron mean free path, and d is the distance between scattering interfaces which is the thickness of a film, the width (or height) of an interconnect line, or the average distance between grain boundaries. Consequently, in the limit of narrow interconnect lines, metals with low $\rho_0\lambda$ products are expected to have a low resistivity and therefore yield interconnects with low signal delay and power consumption [24], [25]. First-principles

simulations predict a room temperature mean free path $\lambda = 5.87$ nm for Ni and a corresponding low $\rho_0 \lambda$ product of 4.07×10^{-16} Ω m² [24], suggesting that Ni has the potential to outperform currently used interconnect metals including Cu, W, and Co, which have 65, 101, and 59% higher predicted $\rho_0\lambda$ products, respectively, where the predicted Co value corresponds to the weighted average parallel and perpendicular to the hexagonal axis. However, reported experimental studies that determine the $\rho_{o}\lambda$ product from measured ρ vs d data indicate that the resistivity scaling and the associated experimental $\rho_0\lambda$ product is often larger than the theoretical prediction, for example by factors of 1.2, 3.9-8.4, and 1.7 for W(110) [26]–[28], Nb [29], and Co(0001) [30], [31]. Therefore, it is important to experimentally measure the resistivity scaling of Ni to validate or correct the theoretical predictions for Ni as a promising interconnect metal. In fact, previous experimental studies on the resistivity size effect in Ni have reported λ values ranging from 16.4-25 nm [32]-[34], which is 2.8-4.3 times larger than the predictions. However, all these studies employ polycrystalline Ni layers where grain boundary scattering contributes to the size effect and may therefore cause inaccuracies in the determined mean free path. This last point motivates the use of epitaxial Ni layers in our study. The key benefit of epitaxial layers is the lack of grain boundaries, allowing direct measurements of the resistance contribution due to surface scattering without the confounding effect from electron grain boundary scattering.

In this report, we determine λ and the product $\rho_o\lambda$ for Ni from the thickness dependence of the resistivity of epitaxial Ni(001) films grown on MgO(001) substrates. X-ray diffraction analyses confirm that the layers are epitaxial, with Ni[001] || MgO[001] and Ni[100] || MgO[100]. The resistivity is measured *in situ* and *ex situ* at 295 and 77 K as a function of *d*, and is described within the semi-classical framework of the FS model yielding a room temperature $\lambda = 26 \pm 2$ nm which is slightly larger than the range from previous experimental studies on polycrystalline Ni layers. The corresponding $\rho_o\lambda = 18.3 \times 10^{-16} \,\Omega \text{m}^2$ is 4.5 times larger than theoretically predicted, indicating that Ni is less promising as an interconnect metal than envisioned.

The authors acknowledge funding from SRC under task 2881, the NY State Empire State Development's Division of Science, Technology and Innovation (NYSTAR) through Focus Center-NY–RPI Contract C150117, and the NSF under grant No. 1740271 and 1712752.

The authors are from The Department of Materials Science and Engineering, Rensselaer Polytechnic Institute, 110 8th St, Troy, NY 12180, USA.

II. PROCEDURE

Ni(001) layers were deposited by magnetron sputtering on MgO(001) substrates in a three-chamber ultrahigh vacuum deposition and analysis system with a base pressure of 10⁻⁹ Torr [35], [36]. The substrates were ultrasonically cleaned in consecutive baths of trichloroethylene, acetone, isopropanol, and deionized water, mounted onto a Mo holder with colloidal silver paint and introduced into the vacuum system via a load lock. Prior to deposition, all substrates were degassed at 1000 °C for 1 hour, and then cooled to the deposition temperature of 200 °C. Deposition was done in 5 mTorr 99.999% pure Ar with a fixed power of 200 W applied to a 99.95% pure 5-cmdiameter Ni target which was facing the substrate at a distance of 9 cm, yielding a deposition rate of 0.07 nm/s. The deposition time was varied to obtain a set of samples with nominal Ni film thicknesses ranging from 5 to 100 nm. After deposition, films were allowed to cool to room temperature in vacuum, followed by in situ transfer to an analysis chamber for electrical transport measurements with an *in situ* linear four-point-probe which was operated with a current of 1 - 100 mA [35]. Measurements at 77 K were taken with an ex situ four-point-probe by submerging each sample in liquid nitrogen after removal from the load-lock that was vented with dry N2. Ex situ room-temperature resistivity measurements were taken with the identical fourpoint-probe after warming the samples up using a continuous flux of N2 gas.

X-ray diffraction and reflectivity (XRR) analyses were performed using a Panalytical X'pert PRO MPD system with a Cu source. θ -2 θ scans, ω -rocking curves, and XRR analyses were acquired using a parabolic mirror which yields a source divergence of <0.055°. Pole figures were acquired using a polycapillary lens as the primary optic, providing a point source with quasi-parallel Cu K $_{\alpha}$ X-rays with a divergence of less than 0.3°. The diffracted beam path for all scans consisted of a 0.27° parallel-plate collimator backed by a scintillation point detector. Fitting of the XRR spectra was done using the recursive theory by Parratt, assuming a Gaussian distribution to model the surface and interface roughnesses, and fixing the densities of the Ni layer and the native NiO surface oxide to the reported bulk values of 8.9 and 6.67 g/cm³, respectively [37], [38].

III. RESULTS AND DISCUSSION

Fig. 1 shows representative X-ray diffraction and XRR results from a 96.9-nm-thick Ni(001)/MgO(001) layer. The diffractogram in Fig. 1(a) is a section of a θ -2 θ scan, plotted from 50.5° to 53.5°. It shows the Ni 002 reflection at 2 θ = 51.94°, which is the only film peak that can be detected over the entire measured range, indicating a 001 layer orientation and an out-of-plane lattice constant of 0.3518 nm which is within the previously reported range for Ni of 0.3516 to 0.3528 nm [39], [40]. The full width at half maximum (FWHM) of the Ni 002 peak is 0.50°, corresponding to an out-of-plane coherence length [41] of 20 nm, which is five times smaller than the layer thickness and suggests local strain variations and/or low angle grain boundaries in the Ni film. Fig. 1(b) is an ω -

rocking curve of the Ni 002 reflection. The peak width of 3.0° is comparable to the 1.8-3.3° reported for Cu(001) on MgO(001) [8], [42] but is 11 and 17 times larger than the 0.27° and 0.18° reported for W(001)[41] and Ag(001)[43] on MgO(001), respectively. The relatively wide peak indicates deviations from perfect crystallinity with an in-plane coherence length of 3.4 nm which implies the presence of strain fields and/or small angle grain boundaries that lead to a 3° spread in the mosaic tilts. Fig. 1(c) is a pole figure taken at a constant 2θ = 44.415° of the Ni 111 reflection. It shows four peaks at the tilt angle $\chi = 55 \pm 2^{\circ}$ and polar angles $\phi = 0^{\circ}$, 90°, 180°, and 270°, indicating a single epitaxial Ni domain. A corresponding scan of the MgO 111 reflections (not shown), confirms in-plane alignment of the Ni <100> with the MgO <100> directions, epitaxial layer-substrate yielding the relationship: Ni[001] MgO[001] and Ni[100] MgO[100], which is in agreement with previous reports on the epitaxial growth of Ni on MgO(001) [44]–[48], and is similar to the reported epitaxy of Cu on MgO(001) [42]. We note here that our deposition temperature of 200 °C is at the upper end of the reported range for good quality Ni epitaxial growth on MgO(001) [48] and may be the reason for the large widths of the Ni 002 reflection in 2θ and ω .

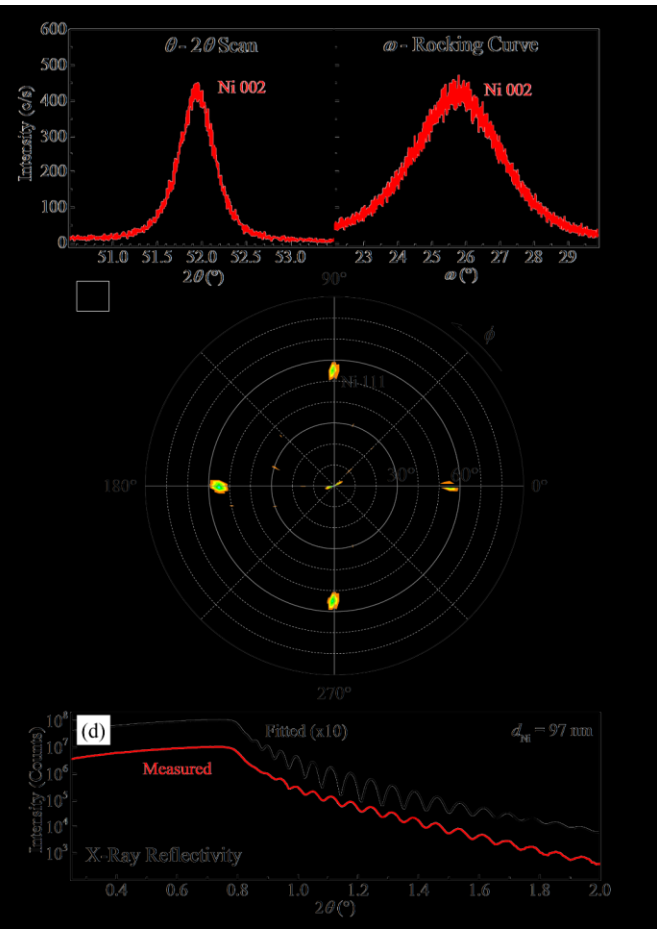


Fig. 1. Representative (a) θ -2 θ scan, (b) 002 ω -rocking curve, (c) 111 pole figure, and (d) XRR scan including the result from curve fitting (black), from an epitaxial Ni(001)/MgO(001) layer with thickness d = 96.9 nm.

Fig. 1(d) shows a representative XRR curve from the same Ni(001) film. The measured intensity is plotted on a logarithmic

scale vs the scattering angle $2\theta = 0.25 - 2.00^{\circ}$. The black line is the result from curve fitting to the experimental measurement and is offset by a factor 10 for clarity. It provides values for the film thickness $d_{\rm Ni} = 96.9 \pm 0.5$ nm and the NiO surface oxide thickness $d_{\rm NiO} = 0.5 \pm 0.3$ nm. The equivalent Ni metal thickness within the NiO layer is 0.2 nm, which corresponds to approximately one monolayer of Ni that is consumed during surface oxidation. That corresponds to 0.2% of the as-deposited Ni and indicates that the as-deposited in situ thickness $d_{\rm Ni} = 97.1$ nm is 0.2 nm larger than the measured thickness. This thickness correction is included when determining the *in situ* film resistivity, as discussed below. Curve fitting also provides values for the root-mean-square roughness of 2.2 ± 0.3 , 2.3 ± 0.2 , and 1.2 ± 0.3 nm for the NiO surface and the NiO-Ni and Ni-MgO interfaces, respectively.

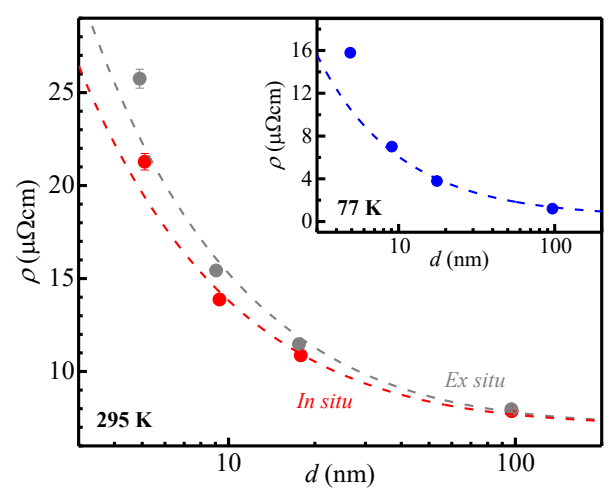


Fig. 2. Resistivity ρ of epitaxial Ni(001)/MgO(001) films vs thickness d, measured in situ (red) and ex situ (gray) in vacuum and air at 295 K, and immersed in liquid N₂ at 77 K (inset, blue). Curves are from data fitting using the FS model.

Similar analyses are done for all samples in this study, showing that they are epitaxial Ni(001) layers with *ex situ* measured metallic Ni thicknesses of $d_{\text{Ni}} = 17.6 \pm 0.4$, 9.1 ± 0.1 , and 4.9 ± 0.1 nm, surface oxides that are 0.5 ± 0.3 nm thick, and resulting *in situ* layer thicknesses $d_{\text{Ni}} = 17.9$, 9.3, and 5.1 nm.

Fig. 2 is a plot of the Ni(001) film resistivity as a function of thickness d_{Ni} measured both in situ and ex situ at 295 K. The in situ measured ρ for the thickest layer with $d_{Ni} = 97.1$ nm is 7.86 \pm 0.02 $\mu\Omega$ cm, which is 12% higher than the reported bulk Ni resistivity $\rho_0 = 7.04 \, \mu\Omega \text{cm}$ [49]–[51]. This deviation is attributed to a resistivity contribution from electron scattering at surfaces which, based on the analysis below, adds 0.78 $\mu\Omega cm$ to ρ_0 for $d_{Ni} = 97.1$ nm. Correspondingly, a contribution to the resistivity from possible residual crystalline defects is $\leq 2\%$, which cannot be detected within our experimental uncertainty. The measured resistivity increases to $\rho = 10.87 \pm 0.06$, 13.87 \pm 0.15, and 21.28 \pm 0.45 $\mu\Omega$ cm as the layer thickness decreases to $d_{Ni} = 17.9, 9.3,$ and 5.1 nm. The plot in Fig. 2 also shows the ex situ resistivity measured after air exposure of the same Ni samples. The ex situ and in situ resistivities are nearly identical for $d_{Ni} = 97$ nm, with an ex situ value of $\rho = 7.97 \pm 0.02 \,\mu\Omega$ cm. However, the thinner Ni(001) layers show a higher resistivity

after air exposure, with $\rho = 11.47 \pm 0.07$, 15.43 ± 0.18 , and $25.75 \pm 0.51 \,\mu\Omega$ cm for $d_{\text{Ni}} = 17.6, 9.1, \text{ and } 4.9 \text{ nm}, \text{ respectively}.$ Note, these latter d_{Ni} values are the measured metallic Ni thickness after surface oxidation and are 0.2-0.3 nm smaller than for the as-deposited layers. The resistivity of the nominally 5-nm-thick Ni(001) layer increases by 21% during air exposure. However, this increase becomes less pronounced with increasing d_{Ni} , indicating that the resistivity increase upon airexposure is a surface effect. Therefore, we attribute this increase to a decrease in the Ni(001) surface specularity upon surface oxidation, similar to what has been reported for Cu [5], [6], [9], [52], Co [31], and Nb [29]. We note that air exposure for an extended time of 690 hours does not result in any detectable change in the resistivity, indicating that roomtemperature Ni oxidation progresses slowly after the initial surface oxidation of approximately one Ni monolayer.

The inset of Fig. 2 shows the measured resistivity at 77 K. The values increase with decreasing thickness from $\rho=1.20\pm0.01$ to 3.79 ± 0.03 , 7.01 ± 0.10 , and 15.79 ± 0.31 $\mu\Omega$ cm for $d_{\rm Ni}=96.9$, 17.6, 9.1, and 4.9 nm, respectively. The resistivity of the sample with $d_{\rm Ni}=96.9$ nm is 2.3 times larger than the reported bulk resistivity $\rho_{\rm o}=0.52$ $\mu\Omega$ cm of Ni at 77 K [49], [51]. This deviation has a similar absolute magnitude as for the 295 K data and is attributed to electron-surface scattering which yields a predicted increase by a factor of 2.6 from the curve fitting procedure described in the following.

The dashed lines in Fig. 2 are obtained from data fitting of the three datasets using the semiclassical framework by Fuchs and Sondheimer [17], [18], as described in the following. A well-known challenge in this approach is the interdependency of the two parameters of the FS model, that is the surface specularity p and the bulk mean free path λ [28], [31], [53]. More specifically, for any choice of p within the physical constraint $0 \le p \le 1$, a value for λ can be found with $\lambda_{\min} \le \lambda \le$ ∞ such that the model predicts a ρ vs d curve that matches the measured data, where λ_{min} is a lower bound for the mean free path consistent with a specific ρ vs d dataset. As a first step, we perform data fitting of the ex situ resistivity (gray data points in Fig. 2) assuming completely diffuse electron scattering at both the upper and lower film surfaces $(p_1 = p_2 = 0)$ and fixing the bulk resistivity to the known room-temperature $\rho_0 = 7.04$ $\mu\Omega$ cm. Thus, the only free fitting parameter in this approach is λ , which corresponds to the lower-bound of possible mean free paths and is determined to be $\lambda_{min} = 26 \pm 2$ nm. The resulting gray dashed line describes the measured data well but underestimates the resistivity of the thinnest $d_{Ni} = 4.9$ nm layer. The data point of this thinnest layer has the largest error bar σ and therefore the least importance during the fitting procedure that uses a common $1/\sigma^2$ weighting. A similar underestimation is also observed for our *in situ* and low-temperature data in Fig. 2 and has also previously been reported for Ru [30], [53], Co [30], [31], Cu [54], [55], W [27], and Nb [29] layers with d <10 nm, and has been attributed to an increasing effect of surface roughness [54] or the breakdown of the FS model at small dimensions [27], [56].

We attribute the resistivity increase between *in situ* to *ex situ* measurements to a decrease in the specularity of electron

surface scattering. Therefore, as a second step, we fit the in situ data using a fixed $\lambda = 26$ nm and use the specularity p_1 of the Ni-vacuum interface as the free fitting parameter. This yields p_1 = 0.3 ± 0.1 and the red dashed line in Fig. 2. Similarly, data fitting of the resistivity at 77 K is done with a fixed $\rho_0 = 0.52$ μΩcm [49], [51] and assuming completely diffuse surface scattering $(p_1 = p_2 = 0)$ as the samples are exposed to atmosphere prior to submersion in liquid nitrogen. This yields $\lambda_{77K} = 350 \pm 20$ nm and the blue dashed line in the inset of Fig. 2. This bulk mean free path is more than an order of magnitude larger than at room temperature, which is expected because of the lower electron-phonon scattering rate. To explore this effect more quantitatively, we use the λ values from our data fitting to determine the product $\rho_0 \lambda = 18.3 \times 10^{-16} \ \Omega \text{m}^2$ at room temperature and $\rho_0 \lambda = 18.2 \times 10^{-16} \,\Omega\text{m}^2$ at 77 K. These values are identical within experimental uncertainty, suggesting that $\rho_0 \lambda$ is temperature-independent, as expected from a classical transport description. However, our $\rho_0\lambda$ value is 4.5 times larger than the theoretically predicted $4.07 \times 10^{-16} \Omega m^2$ [24], indicating that the resistivity size effect in Ni is significantly stronger than the first-principles calculations suggest. The $\rho_0\lambda$ product for Ni is also 1.5 to 3.6 times larger than the reported $\rho_0\lambda$ products for Cu $(6.7\times10^{-16} \ \Omega \text{m}^2)$ [7], W(110) $(10.1\times10^{-16} \ \Omega \text{m}^2)$ [26], Co(0001) $(12.2\times10^{-16} \Omega \text{m}^2)$ [30], [31], and Ru(0001) $(5.06\times10^{-16} \Omega \text{m}^2)$ [30], [53], such that we conclude that Ni is not a promising metal for high-conductivity narrow interconnect lines.

IV. CONCLUSIONS

The measured electrical resistivity of epitaxial Ni(001)/MgO(001) layers with d = 5-100 nm is well described with the Fuchs-Sondheimer model with a bulk electron mean free path $\lambda = 26 \pm 2$ and 350 ± 20 nm at 295 and 77 K, respectively. Air-exposure causes a resistivity increase by up to 21% which is attributed to a transition from partially specular $(p_1 = 0.3)$ electron scattering at the Ni-vacuum interface to completely diffuse $(p_1 = 0)$ scattering at the oxidized Ni surface. The data indicates a temperature-independent product $\rho_0 \lambda =$ $18.3 \times 10^{-16} \Omega m^2$ which is 4.5 times larger than a previous first principles prediction. Consequently, Ni is (opposite to this prediction) not promising as metal for next generation interconnect technologies.

REFERENCES

- [1] J. Kelly, J. H.-C. Chen, H. Huang, C. K. Hu, E. Liniger, R. Patlolla, B. Peethala, P. Adusumilli, H. Shobha, T. Nogami, T. Spooner, E. Huang, D. Edelstein, D. Canaperi, V. Kamineni, F. Mont, and S. Siddiqui, "Experimental study of nanoscale Co damascene BEOL interconnect structures," in 2016 IEEE International Interconnect Technology Conference / Advanced Metallization Conference (IITC/AMC), May. 2016, pp. 40–42, doi: 10.1109/IITC-AMC.2016.7507673.
- [2] J. S. Chawla, S. H. Sung, S. A. Bojarski, C. T. Carver, M. Chandhok, R. V. Chebiam, J. S. Clarke, M. Harmes, C. J. Jezewski, M. J. Kobrinski, B. J. Krist, M. Mayeh, R. Turkot, and H. J. Yoo, "Resistance and electromigration performance of 6 nm wires," in 2016 IEEE International Interconnect Technology Conference / Advanced Metallization Conference (IITC/AMC), May. 2016, pp. 63–65, doi: 10.1109/IITC-AMC.2016.7507682.
- [3] S. M. Rossnagel and T. S. Kuan, "Alteration of Cu conductivity in the size effect regime," J. Vac. Sci. Technol. B Microelectron. Nanom. Struct., vol. 22, no. 1, p. 240, 2004, doi: 10.1116/1.1642639.

- [4] J. J. Thomson, "On the theory of electric conduction through thin metallic films," *Proc. Camb. Philol. Soc.*, vol. 11, pp. 120–123, 1901.
- [5] P. Y. Zheng, R. P. Deng, and D. Gall, "Ni doping on Cu surfaces: Reduced copper resistivity," *Appl. Phys. Lett.*, vol. 105, no. 13, p. 131603, Sep. 2014, doi: 10.1063/1.4897009.
- [6] P. Zheng, T. Zhou, and D. Gall, "Electron channeling in TiO₂ coated Cu layers," *Semicond. Sci. Technol.*, vol. 31, no. 5, p. 055005, May 2016, doi: 10.1088/0268-1242/31/5/055005.
- [7] J. S. Chawla, F. Gstrein, K. P. O'Brien, J. S. Clarke, and D. Gall, "Electron scattering at surfaces and grain boundaries in Cu thin films and wires," *Phys. Rev. B*, vol. 84, no. 23, p. 235423, Dec. 2011, doi: 10.1103/PhysRevB.84.235423.
- [8] J. S. Chawla and D. Gall, "Specular electron scattering at single-crystal Cu(001) surfaces," *Appl. Phys. Lett.*, vol. 94, no. 25, p. 252101, Jun. 2009, doi: 10.1063/1.3157271.
- [9] E. Milosevic and D. Gall, "Copper Interconnects: Surface State Engineering to Facilitate Specular Electron Scattering," *IEEE Trans. Electron Devices*, vol. 66, no. 6, pp. 2692–2698, Jun. 2019, doi: 10.1109/TED.2019.2910500.
- [10] A. F. Mayadas and M. Shatzkes, "Electrical-Resistivity Model for Polycrystalline Films: the Case of Arbitrary Reflection at External Surfaces," *Phys. Rev. B*, vol. 1, no. 4, pp. 1382–1389, Feb. 1970, doi: 10.1103/PhysRevB.1.1382.
- [11] M. César, D. Gall, and H. Guo, "Reducing Grain-Boundary Resistivity of Copper Nanowires by Doping," *Phys. Rev. Appl.*, vol. 5, no. 5, p. 054018, May 2016, doi: 10.1103/PhysRevApplied.5.054018.
- [12] M. César, D. Liu, D. Gall, and H. Guo, "Calculated Resistances of Single Grain Boundaries in Copper," *Phys. Rev. Appl.*, vol. 2, no. 4, p. 044007, Oct. 2014, doi: 10.1103/PhysRevApplied.2.044007.
- [13] D. Choi, "The electron scattering at grain boundaries in tungsten films," *Microelectron. Eng.*, vol. 122, pp. 5–8, Jun. 2014, doi: 10.1016/j.mee.2014.03.012.
- [14] T.-H. Kim, X.-G. Zhang, D. M. Nicholson, B. M. Evans, N. S. Kulkarni, B. Radhakrishnan, E. A. Kenik, and A.-P. Li, "Large Discrete Resistance Jump at Grain Boundary in Copper Nanowire," *Nano Lett.*, vol. 10, no. 8, pp. 3096–3100, Aug. 2010, doi: 10.1021/nl101734h.
- [15] J. M. Rickman and K. Barmak, "Simulation of electrical conduction in thin polycrystalline metallic films: Impact of microstructure," *J. Appl. Phys.*, vol. 114, no. 13, p. 133703, Oct. 2013, doi: 10.1063/1.4823985.
- [16] N. A. Lanzillo, H. Dixit, E. Milosevic, C. Niu, A. V Carr, P. Oldiges, M. V Raymond, J. Cho, T. E. Standaert, and V. K. Kamineni, "Defect and grain boundary scattering in tungsten: A combined theoretical and experimental study," *J. Appl. Phys.*, vol. 123, no. 15, p. 154303, Apr. 2018, doi: 10.1063/1.5027093.
- [17] K. Fuchs and N. F. Mott, "The conductivity of thin metallic films according to the electron theory of metals," *Math. Proc. Cambridge Philos. Soc.*, vol. 34, no. 01, p. 100, Jan. 1938, doi: 10.1017/S0305004100019952.
- [18] E. H. Sondheimer, "The mean free path of electrons in metals," Adv. Phys., vol. 1, no. 1, pp. 1–42, Jan. 1952, doi: 10.1080/00018735200101151.
- [19] A. F. Mayadas, M. Shatzkes, and J. F. Janak, "Electrical resistivity model for polycrystalline films: The case of specular reflection at external surfaces," *Appl. Phys. Lett.*, vol. 14, no. 11, pp. 345–347, Jun. 1969, doi: 10.1063/1.1652680.
- [20] Y. Namba, "Resistivity and Temperature Coefficient of Thin Metal Films with Rough Surface," *Jpn. J. Appl. Phys.*, vol. 9, no. 11, pp. 1326–1329, Nov. 1970, doi: 10.1143/JJAP.9.1326.
- [21] Y. Ke, F. Zahid, V. Timoshevskii, K. Xia, D. Gall, and H. Guo, "Resistivity of thin Cu films with surface roughness," *Phys. Rev. B*, vol. 79, no. 15, p. 155406, Apr. 2009, doi: 10.1103/PhysRevB.79.155406.
- [22] P. Y. Zheng, T. Zhou, B. J. Engler, J. S. Chawla, R. Hull, and D. Gall, "Surface roughness dependence of the electrical resistivity of W(001) layers," J. Appl. Phys., vol. 122, no. 9, p. 095304, Sep. 2017, doi: 10.1063/1.4994001.
- [23] T. Zhou, P. Zheng, S. C. Pandey, R. Sundararaman, and D. Gall, "The electrical resistivity of rough thin films: A model based on electron reflection at discrete step edges," *J. Appl. Phys.*, vol. 123, no. 15, p. 155107, Apr. 2018, doi: 10.1063/1.5020577.
- [24] D. Gall, "Electron mean free path in elemental metals," J. Appl. Phys., vol. 119, no. 8, p. 085101, Feb. 2016, doi: 10.1063/1.4942216.
- [25] D. Gall, "Metals for Low-Resistivity Interconnects," in 2018 IEEE International Interconnect Technology Conference (IITC), Jun. 2018, pp. 157–159, doi: 10.1109/IITC.2018.8456810.
- [26] P. Zheng and D. Gall, "The anisotropic size effect of the electrical

- resistivity of metal thin films: Tungsten," *J. Appl. Phys.*, vol. 122, no. 13, p. 135301, Oct. 2017, doi: 10.1063/1.5004118.
- [27] D. Choi, X. Liu, P. K. Schelling, K. R. Coffey, and K. Barmak, "Failure of semiclassical models to describe resistivity of nanometric, polycrystalline tungsten films," *J. Appl. Phys.*, vol. 115, no. 10, p. 104308, Mar. 2014, doi: 10.1063/1.4868093.
- [28] D. Choi, C. S. Kim, D. Naveh, S. Chung, A. P. Warren, N. T. Nuhfer, M. F. Toney, K. R. Coffey, and K. Barmak, "Electron mean free path of tungsten and the electrical resistivity of epitaxial (110) tungsten films," *Phys. Rev. B*, vol. 86, no. 4, p. 045432, Jul. 2012, doi: 10.1103/PhysRevB.86.045432.
- [29] E. Milosevic, S. Kerdsongpanya, M. E. McGahay, B. Wang, and D. Gall, "The Resisitivity Size Effect in Epitaxial Nb(001) and Nb(011) Layers," *IEEE Trans. Electron Devices*, vol. 66, no. 8, pp. 3473-3478, Aug. 2019, doi: 10.1109/TED.2019.2924312.
- [30] E. Milosevic, S. Kerdsongpanya, and D. Gall, "The Resistivity Size Effect in Epitaxial Ru(0001) and Co(0001) Layers," in 2018 IEEE Nanotechnology Symposium (ANTS), Nov. 2018, pp. 1–5, doi: 10.1109/NANOTECH.2018.8653560.
- [31] E. Milosevic, S. Kerdsongpanya, M. McGahay, A. Zangiabadi, and K. Barmak, "Resistivity Scaling and Electron-Surface Scattering in Epitaxial Co(0001) Layers," *J. Appl. Physics*, vol. 125, no. 24, p. 245105, June 2019, doi: 10.1063/1.5086458.
- [32] A. H. Eid, S. Mahmoud, M. S. Elmanharawy, and S. T. Badr, "Size-dependent electrical conduction of thin nickel films," *Czechoslov. J. Phys.*, vol. 29, no. 4, pp. 451–459, Apr. 1979, doi: 10.1007/BF01596555.
- [33] B. C. Johnson, "Electrical resistivity of copper and nickel thin-film interconnections," J. Appl. Phys., vol. 67, no. 6, pp. 3018–3024, Mar. 1990, doi: 10.1063/1.345424.
- [34] M. A. Angadi and L. A. Udachan, "Electrical properties of thin nickel films," *Thin Solid Films*, vol. 79, no. 2, pp. 149–153, May 1981, doi: 10.1016/0040-6090(81)90272-8.
- [35] M. E. McGahay and D. Gall, "Conductive surface oxide on CrN(001) layers," *Appl. Phys. Lett.*, vol. 114, no. 13, p. 131602, 2019, doi: 10.1063/1.5091034.
- [36] B. Wang, S. Kerdsongpanya, M. E. McGahay, E. Milosevic, P. Patsalas, and D. Gall, "Growth and properties of epitaxial Ti 1- x Mg x N(001) layers," *J. Vac. Sci. Technol. A*, vol. 36, no. 6, p. 061501, Nov. 2018, doi: 10.1116/1.5049957.
- [37] B. L. Zink, M. Manno, L. O'Brien, J. Lotze, M. Weiler, D. Bassett, S. J. Mason, S. T. B. Goennenwein, M. Johnson, and C. Leighton, "Efficient spin transport through native oxides of nickel and permalloy with platinum and gold overlayers," *Phys. Rev. B*, vol. 93, no. 18, p. 184401, May 2016, doi: 10.1103/PhysRevB.93.184401.
- [38] S. L. Medway, C. A. Lucas, A. Kowal, R. J. Nichols, and D. Johnson, "In situ studies of the oxidation of nickel electrodes in alkaline solution," *J. Electroanal. Chem.*, vol. 587, no. 1, pp. 172–181, 2006, doi: 10.1016/j.jelechem.2005.11.013.
- [39] Swanson and Tatge, "Standard X-Ray Diffraction Patterns," Natl. Bur. Stand., vol. 1, no. 13, p. 539, 1953.
- [40] V. S. Kogan and A. S. Bulatov, "The Temperature Dependence fo the Isotope Effect in the Nickel Lattice," Zh. Eksp. Teor, Fiz, vol. 42, p. 1499, 1962.
- [41] P. Zheng, B. D. Ozsdolay, and D. Gall, "Epitaxial growth of tungsten layers on MgO(001)," J. Vac. Sci. Technol. A Vacuum, Surfaces, Film., vol. 33, no. 6, p. 061505, Nov. 2015, doi: 10.1116/1.4928409.
- [42] J. M. Purswani, T. Spila, and D. Gall, "Growth of epitaxial Cu on MgO(001) by magnetron sputter deposition," *Thin Solid Films*, vol. 515, no. 3, pp. 1166–1170, Nov. 2006, doi: 10.1016/j.tsf.2006.07.142.
- [43] J. S. Chawla and D. Gall, "Epitaxial Ag(001) grown on MgO(001) and TiN(001): Twinning, surface morphology, and electron surface scattering," J. Appl. Phys., vol. 111, no. 4, p. 043708, Feb. 2012, doi: 10.1063/1.3684976.
- [44] G. Safran, H. Qiu, M. Adamik, M. Hashimoto, P. B. Barna, H. Maruyama, and A. Kosuge, "Epitaxial growth, structure and properties of Ni films grown on MgO(100) by d.c. bias sputter deposition," *Thin Solid Films*, vol. 241, no. 1–2, pp. 9–11, 2002, doi: 10.1016/0040-6090(94)90385-9.
- [45] H. Qiu, H. Nakai, M. Hashimoto, G. Safran, M. Adamik, P. B. Barna, and E. Yagi, "Epitaxial growth and characterization of Ni films grown on MgO(001) by biased direct-current sputter deposition," *J. Vac. Sci. Technol. A Vacuum, Surfaces, Film.*, vol. 12, no. 5, pp. 2855–2858, 2002, doi: 10.1116/1.578956.
- [46] J. P. McCaffrey, E. B. Svedberg, J. R. Phillips, and L. D. Madsen, "Epitaxial variations of Ni films grown on MgO(0 0 1)," J. Cryst. Growth, vol. 200, no. 3, pp. 498–504, 1999, doi: 10.1016/S0022-0248(98)01403-

- [47] F. Reniers, M. P. Delplancke, A. Asskali, V. Rooryck, and O. Van Sinay, "Glow discharge sputtering deposition of thin films of Ag, Cr, Cu, Ni, Pd, Rh and their binary alloys onto NaCl and MgO experimental parameters and epitaxy," *Appl. Surf. Sci.*, vol. 92, pp. 35–42, 1996, doi: 10.1016/0169-4332(95)00198-0.
- [48] E. B. Svedberg, P. Sandström, J. E. Sundgren, J. E. Greene, and L. D. Madsen, "Epitaxial growth of Ni on MgO(002) 1 × 1: surface interaction vs. multidomain strain relief," Surf. Sci., vol. 429, no. 1, pp. 206–216, 1999, doi: 10.1016/S0039-6028(99)00379-9.
- [49] W. M. Haynes, "Electrical Resistivity of Pure Metals," CRC Handbook of Chemistry and Physics. CRC Press, Boca Raton, Fla., 2014.
- [50] J. W. C. De Vries, "Temperature and thickness dependence of the resistivity of thin polycrystalline aluminium, cobalt, nickel, palladium, silver and gold films," *Thin Solid Films*, vol. 167, no. 1–2, pp. 25–32, Dec. 1988, doi: 10.1016/0040-6090(88)90478-6.
- [51] L. A. Hall, "Survey of electrical resistivity measurements on 16 pure metals in the temperature range 0 to 273 K," *Nat. Bur. Stand. Tech. Note*, vol. 365, p. 20, 1968.
- [52] J. S. Chawla, X. Y. Zhang, and D. Gall, "Epitaxial TiN(001) wetting layer for growth of thin single-crystal Cu(001)," *J. Appl. Phys.*, vol. 110, no. 4, p. 043714, Aug. 2011, doi: 10.1063/1.3624773.
- [53] E. Milosevic, S. Kerdsongpanya, A. Zangiabadi, K. Barmak, K. R. Coffey, and D. Gall, "Resistivity size effect in epitaxial Ru(0001) layers," J. Appl. Phys., vol. 124, no. 16, p. 165105, Oct. 2018, doi: 10.1063/1.5046430.
- [54] Y. P. Timalsina, A. Horning, R. F. Spivey, K. M. Lewis, T.-S. Kuan, G.-C. Wang, and T.-M. Lu, "Effects of nanoscale surface roughness on the resistivity of ultrathin epitaxial copper films," *Nanotechnology*, vol. 26, no. 7, p. 075704, Feb. 2015, doi: 10.1088/0957-4484/26/7/075704.
- [55] H.-D. Liu, Y.-P. Zhao, G. Ramanath, S. P. Murarka, and G.-C. Wang, "Thickness dependent electrical resistivity of ultrathin (<40 nm) Cu films," *Thin Solid Films*, vol. 384, no. 1, pp. 151–156, Mar. 2001, doi: 10.1016/S0040-6090(00)01818-6.
- [56] T. Zhou and D. Gall, "Resistivity scaling due to electron surface scattering in thin metal layers," *Phys. Rev. B*, vol. 97, no. 16, p. 165406, Apr. 2018, doi: 10.1103/PhysRevB.97.165406.